

Article Presented at
International Conference on Metallurgical Coatings and Thin Films
April 22-25 2002, San Diego USA

Investigation of non-hydrogenated DLC:Si prepared by cathodic arc

Othon R. Monteiro⁽¹⁾ and Marie-Paule Delplancke-Ogletree⁽²⁾

*(1) Lawrence Berkeley National Laboratory, University of California,
Berkeley, California 94720*

*(2) Department Métallurgie-Electrochimie, Université Libre de Bruxelles, CP 165
Brussels 1050, Belgium*

March 2002

Contact Author: Dr. Othon R. Monteiro
Lawrence Berkeley National Laboratory
Mail Stop 53-004
One Cyclotron Rd.
Berkeley, CA 94720 USA
e-mail: ORMonteiro@lbl.gov
FAX: (510) 486-4374

This work was supported by the U.S. Department of Energy, under contract No. DE-AC03-76SF00098.

Synthesis, properties and applications of pure and covalently doped DLC films prepared by energetic condensation.

Othon R. Monteiro⁽¹⁾ and Marie-Paule Delplancke-Ogletree⁽²⁾

(1) Lawrence Berkeley National Laboratory
University of California, Berkeley
Berkeley, CA 94720 U.S.A.

(2) Department Métallurgie-Electrochimie,
Université Libre de Bruxelles, CP 165
Brussels 1050, Belgium

Abstract:

Non-hydrogenated DLC films (also referred as ta-C) have been extensively studied and are used for a variety of wear related applications. Alloying DLC with refractory metals and other elements have been shown to be promising techniques to overcome some of the problems associated with pure DLC, such as excessive level of intrinsic stresses and high-temperature stability. The microstructure of DLC:Me in general consists of crystalline metal carbides dispersed in a DLC matrix. In contrary, DLC:Si has an amorphous structure. We have used filtered cathodic arc to prepare DLC:Si up to 6% Si, and have characterized their structure and bonding using microscopy (TEM) and spectroscopy (XPS, NEXAFS). The effect of Si in changing the bonding configuration of the C network is discussed. The microstructure is then correlated to hardness and friction measured by nano-indentation and micro-wear.

Introduction:

In response to the challenges of implementing diamondlike carbon (DLC) films into several applications, there has been extensive work on the addition of alloying elements to DLC in order to enhance their performance. Alloying elements have included refractory metals [1] silicon [2-4] as well as other elements such as N and F. Incorporation of such elements typically leads to improvements in some properties at the expense of others.

Incorporation of Si has resulted in decrease in intrinsic stresses [2,4]. Such stresses can reach values higher than 10 GPa in non-hydrogenated DLC [5], and about 3 GPa in hydrogenated DLC [2]. Although there is a general acceptance that silicon incorporation promotes reduction of internal stresses, the results concerning other properties are not as generally accepted. For instance, hardness of hydrogenated DLC:Si had been reported to be insensitive to the silicon content up to 50% Si [2] or to decrease with increasing Si content [6]. Notice that the hardness of amorphous SiC has been reported to be of around 20 - 25 GPa [7,8], which is reasonably close to that of a-C:H (hydrogenated DLC). Other reported beneficial effects of Si addition are the enhancement in thermal stability [9,10] and improved adhesion when compared to undoped DLC [11]. The coefficient of friction of DLC:Si has also been reported to be less sensitive to environment conditions [12].

Most of the work on silicon additions to DLC has involved hydrogenated films.

Nevertheless two recently published articles have investigated the incorporation of Si in non-hydrogenated DLC using a hybrid sputtering-cathodic arc deposition system [4] or

two cathodic arc deposition systems [3]. The work presented here also focuses in non-hydrogenated DLC:Si prepared by filtered cathodic arc. We use X-ray absorption spectroscopy to investigate the bonding structure in the films, and nanoindentation and nanoscratch tests to evaluate the mechanical and tribological properties of the films.

2.0 Experimental Procedure:

2.1 Deposition of DLC Films

The DLC:Si films have been prepared using two synchronized filtered cathodic plasma sources and a pulsed bias voltage applied to the substrate. The filtered cathodic plasma sources[13] were used: one with a graphite cathode and the other with a silicon cathode. The two sources were triggered simultaneously and the composition of the films controlled by varying the duration of the pulses in each source. During each plasma pulse a thickness corresponding to a fraction of a monolayer of the cathode element was deposited. Therefore we did not expect any stratification in the film.

A pulsed bias voltage was applied to the substrate during each arc pulse. Typical arc current in the plasma sources were 250 A in the carbon source and 150 A in the silicon source. The pulse duration of the carbon source was 5 ms, and the silicon source varied from 0.5 ms to 2.5 ms. The arc frequency was 1 Hz and pulsed bias voltage of -100 V was applied to the substrate with alternating on-periods of $2\text{ }\mu\text{s}$ and off-periods of $6\text{ }\mu\text{s}$.

2.2 Chemical and Structural Characterization

Quantitative chemical composition of the deposited films was obtained by Rutherford Backscattering Spectroscopy using a 1.8 keV He⁺ beam. X-ray absorption spectroscopy (NEXAFS) was used to analyze the bond chemistry of these films. NEXAFS spectra were taken using synchrotron radiation at the beam 7.3.1.1 at the Advanced Light Source. This is a bending magnet beamline that covers the 175 – 1500 eV spectral range, which contains the K-edges of the light elements (B, C, O, N and F), the L-edges of the 3d transition metals and the M_{4,5}-edges of the rare-earths [14]. Graphite and a diamond crystal were used as sample references for the energy calibration. The NEXAFS spectra were taken in a total electron yield mode by measuring the current from the sample to ground.

Transmission electron microscopy was used to characterize the morphology and structure of the films. TEM was carried out in a Phillips CM200 with a PEELS (Parallel Energy Loss Spectroscopy) system and a Topcon 002B with point resolution of 0.19 nm at 200 kV.

2.3 Mechanical and Tribological Characterization

Hardness and elastic modulus of the films were determined by nanoindentation using a Hysitron Picoindenter. The hardness was evaluated from the residual impression of the indenter whereas the modulus was determined from the slope of the load-unload curve at the beginning of the unloading process [15]. Friction coefficient was also determined by using a Hysitron Triboscope measuring the lateral force for different vertical loads. Coefficients of friction were determined using a single-pass scratch test. In this test, a

hard indenter slides along a surface and the induced tangential and normal forces as well as the resulting scratch morphology are measured to obtain the desired properties.

3.0 Results and Discussions:

The Si-content of the DLC:Si used in this work consisted of 3 at%, 5 at% and 6 at%, as determined by RBS. The properties of the DLC:Si are compared with those of undoped DLC films, which were prepared under the same applied bias voltage. The film composition results from a balance between the incident ion currents from the two plasma sources and the sputtering rates of the individual elements (Si and C) due to the incident energetic Si^{n+} and C^+ ions. The mean charge state of the Si^{n+} ions generated by the cathodic arc source is 1.4 (the plasma stream consists of a mixture of about 63% of Si^+ , 35% of Si^{2+} and the balance of Si^{3+}) [16]. Thus the mean energy transferred to the growing film is not exactly equivalent to that transferred when an undoped DLC film is deposited with the same bias voltage. This fact is important to some extent because the properties of undoped DLC strongly depend on the energetics of the deposition. However, since ratio Si:C in the mixed plasma stream is small, the final effect of the difference in charge states and the ion native energy on the energetics of the deposition is not expected to be large.

Transmission electron microscopy of the DLC:Si films demonstrated that the films are amorphous and are under compressive stress. Figure 1 shows a bright field TEM image of a free-standing DLC:Si (5 at%). The wavy pattern seen in Figure 1 is typical of

films under compressive stresses. Electron diffraction patterns indicate the amorphous nature of the films. This result was also supported by X-ray diffraction.

Near-edge X-ray absorption fine structure spectroscopy was performed C_K edge in order to determine the bonding state in the films. Detailed peak identification in NEXAFS is not straightforward. Graphite and diamond samples were used as standards. In addition, we obtained NEXAFS spectra of three undoped DLC films prepared using a pulsed bias voltage of $-100V$ with duty cycles of 0%, 50% and 75% (duty cycle means the percent of the time that the bias was actually applied), and their spectra is shown in Figure 2. No attempt to remove surface contamination was done prior to obtaining the spectra in Figure 2.

The incorporation of impurities (mainly oxygen and hydrogen) during deposition and adsorption during storage and transfer of samples from deposition chamber to analysis chamber can complicate the interpretation of the absorption spectra. Several absorption peaks around the C-K 1s edge have been identified [17-20]. Table I summarizes reported transitions and corresponding energies.

In order to understand the impact of Si additions on bonding, it was necessary characterize the transitions (peaks) seen in Figure 2. The greatest uncertainty regarding peak assignment resides with the peak near 289.1 eV. According to Jaouen et al [19], this peak could be attributed to occurrence of $(O=C-OH)$. An experiment was then carried out to verify whether this is a plausible assignment for the films prepared by FCA. Films

prepared at similar bias voltage of -100V but with different duty cycle were prepared, and the NEXAFS spectra obtained from these films are presented in Figure 2. Since increasing duty cycle leads to increases in sp^3 content in the film, and the 289 eV peaks increase accordingly, we conclude that the peak at 289 eV is in fact related with σ bonds, and not with $\text{O}=\text{C}-\text{OH}$.

The effect of adding Si to the ta-C can be directly seen from Figure 3, where the spectra obtained from a ta-C and from three DLC:Si samples (3, 5 and 6at%) are plotted. The increase in the intensity of the peak at 289 eV when Si is incorporated in the film suggests that there is an increase in sp^3 content. The ratio $I(289\text{ eV})/I(285\text{ eV})$ can be used to determine the sp^3 content in undoped amorphous carbon films [20]. Extending this idea to doped films, we conclude that the sp^3 content decreases in the following order: $3\text{at\%} > 5\text{at\%} > 6\text{at\%}$. A complete understanding of the bond structure of such films requires further investigation.

Hardness values of the DLC:Si films obtained at several loads (depths) are shown in Figure 4. The hardness of optimized undoped DLC films prepared by filtered cathodic arc under the conditions used here was 72 GPa . Thus, adding 3 at\% Si leads to a small decrease in hardness. Hardness decreases as the silicon content increases, as expected due to the weaker Si-C bond as compared to the C-C bond. The large decrease in internal stress is observed with increasing Si content [4] has been correlated with this difference in bond strength. Elastic modulus (measured from nanoindentation tests but not plotted here) shows similar dependence on the silicon content as hardness.

In the remaining of this article we report on the friction coefficient (COF) of the DLC:Si films. The scratch tests here consisted of single-pass tests carried out at several loads from 50 to 400 μN . The total travel of the indenter in each test was 20 μm . Average values of the COFs were calculated for each load by considering the data obtained within the interval 10 – 17 μm . This interval was chosen because in several of the tests there was an obvious transient when the COF was slightly lower at the beginning of the test. These average values are plotted in Figure 5 for the three silicon concentrations.

The observed dependence of COF on the applied load can be explained on the basis of two components that affect its magnitude: adhesion and plowing. The COF plotted in Figure 5 is the overall COF, defined by the ratio of the tangential force to the normal force, but this one can be divided in two components:

$$\mu = \frac{F_T}{F_N} = \mu_a + \mu_p$$

where μ_a is related to the interfacial friction coefficient, and μ_p correlates with the resistance of the indenter to plow into the material

At the highest loads (300 and 400 μN), the friction coefficient increases with the Si content. This result can be explained based on the expression for COF (μ). At high loads the importance of the plowing component is expected to be larger than the interfacial friction. The hardness of DLC:Si decreases with increasing Si, as shown in Figure 4,

and the resistance of the indenter to plow into the material is directly related to the hardness. At the smallest loads (50 and 100 μN), when the interfacial friction is more relevant than the plowing term, there appears to be a minimum at 5 at% Si, and at the intermediate loads, the situation is not well defined. The behavior at small and intermediate loads cannot be explained on the basis of the experimental data presented here.

4.0 Summary and Conclusions:

DLC:Si films were prepared using dual source filtered cathodic arc plasma, and the mechanical and tribological properties of the films were measured. Small additions of Si lead to significant decrease in intrinsic stresses, but the hardness is still higher than 60 GPa. Further increase in Si content reduced the hardness to about 45 GPa, which is still significantly higher than SiC.

The observed coefficient of friction increases with increasing applied load for small loads, and level off for higher loads. This can be explained on the basis of the increasingly important contribution of the plowing phenomenon to the COF because at higher loads the material volume to be removed is larger. Plowing of the substrate can also explain the dependence of the COF on the Si content for high loads.

Near Edge X-ray Absorption Fine Structure Spectroscopy was used to analyze the bonding. Addition of Si results in films with higher content of sp^3 (as inferred from the

increase in intensity of peak at 289) and the decrease in the observed hardness can be associated with the weaker C-Si bond when compared to C-C bond.

Acknowledgements:

The authors would like to thank the Computer Mechanics Laboratory at the University of California, Berkeley. This work was supported by the Director, Office of Science, Office of Basic Energy Sciences, of the U.S. Department of Energy under Contract No. DE-AC03-76SF00098.

References:

1. M. P. Delplacke-Ogletree and O. R. Monteiro, Surface and Coatings Technology 108-109 (1998) 484-488.
2. A. L. Baia-Neto, R. A. Santos, F. L. Freire Jr., S. S. Camargo Jr., R. Carius, F. Finger, W. Beyer, Thin Solid Films 293 (1997) 206-211.
3. J. R. Shi, X. Shi, Z. Sun, E. Liu, H. S. Yang, L. K. Cheah and X. Z. Jin, J. Phys.: Condens. Matter 11 (1999) 5111-5118.
4. C. S. Lee, K. R. Lee, K. Y. Eun, K. H. Yoon, J. H. Han, Diamond and Related Materials 11 (2002) 198-203
5. O. R. Monteiro, J. W. Ager III, D. H. Lee, R. Yu Lo, K. C. Walter and M. Natasi; J. Appl. Phys. 88(5) (2000) 2395-2399.
6. J. F. Zhao, P. Lemoine, Z. H. Liu, J. P. Quinn, P. Maguire and J. A. McLaughlin, Diamond and Related Materials 10 (2001) 1070-1075
7. J. R. Shi, X. Xhi, Z. Sun, E. Liu, B. K. Tay and X.Z. Jin; Inter. J. Modern Phys. B, 14 (2-3) (1997) 213 - 219
8. H. Lieste, U. Dambacher, S. Ulrich and H. Holleck Surface and Coatings Technology 116-119 (1999) 313-320
9. W. J. Wu and M. H. Hon, Surface and Coatings Technology 111 (1999) 134-140
10. S. S. Camargo Jr, R. A. Santos, A. L. Baia-Neto, R. Carius and F. Finger, Thin Solid Films 332 (1998) 130-135
11. J. C. Damansceno, S. S. Camargo Jr, F. L. Freire Jr, and R. Carius Surface and Coatings Technology 133 (2000) 247-252
12. C. Donnet Surface and Coatings Technology 100-101 (1998) 180-186
13. R. A. MacGill, M. R. Dickinson, A. Anders, O. R. Monteiro and I. G. Brown Rev. Sci. Instrum. 69 (2) (1998) 801-803
14. J. Stohr and S. Anders, IBM J. Res. Develop. 44 (2000) 535
15. W. C. Oliver and G. M. Pharr, J. Materials Res. 7(6) (1992) 1564-1583
16. J. E. Galvin, I. G. Brown, R. A. MacGill, Rev. Sci. Instrum. 61 (1) (1990) 583-585

17. I. Jimenez, D. G. J. Sutherland, T. van Buuren, J. A. Carlisle, L. T. Terminello, F. J. Himpsel; Phys. Rev. B 57(20) (1998) 13167-13174
18. C. Lenardi, P. Piseri, V. Briois, C. E. Bottani, A. Li Bassi and P. Milani J. Appl. Phys. 85(10), (1999) 7159-7167
19. M. Jaouen, G. Tourllilon, J. Delafond, N. Junqua, G. Hug, Diamond and Related Materials 4 (1995) 200-206
20. J. Diaz, S. Anders, X. Zhou, E. J. Moler, S. A. Kellar and Z. Hussain Phys. Rev. B 64 (2001) 125204 1-19

Table I:

Energy (eV)	Transition	Reference
284.9 – 285.6	$1s \rightarrow \pi^*$ of sp^2 (C=C)	[17-19]
286.8	$1s \rightarrow \pi^*$ of sp^2 (C=O)	[17,19]
287.8	$1s \rightarrow \sigma^*$ of sp^3 (C-H)	[17,19]
288.5	$1s \rightarrow \pi^*$ (O=C—OH)	[19]
288.8	Excitonic process (like in diamond)	[18]
289	Resonance $1s \rightarrow \sigma^*$ of sp^3 (C-C)	[17,20]
290 - 310	$1s \rightarrow \sigma^*$ of sp^3 (C-C) broadened because it is amorphous	[17]

List of Figures:

Figure 1: Transmission electron microscope image of a free standing DLC:Si (5 at%).

The wavy appearance is characteristic of a film under compressive stress

Figure 2: NEXAFS spectra of undoped DLC films prepared using filtered cathodic arc and applied bias voltage of -100 V. The films were prepared at three different duty cycles (0 %, 50 % and 75 %), and the sp^3 content increases with increasing duty cycle.

Figure 3, NEXAFS spectra of undoped DLC and DLC:Si (5 at%) prepared using filtered cathodic arc and applied bias voltage of -100 V.

Figure 4: Hardness of the DLC:Si films obtained at several loads.

Figure 5: COF average values of DLC:Si obtained at different applied loads.

Figure 1:

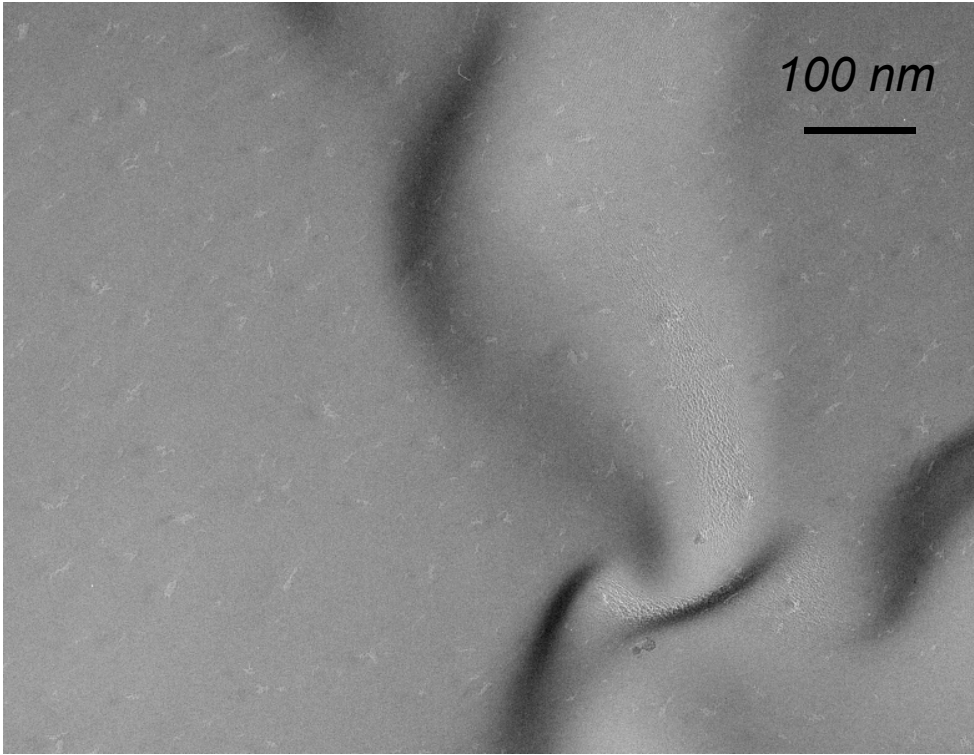


Figure 2:

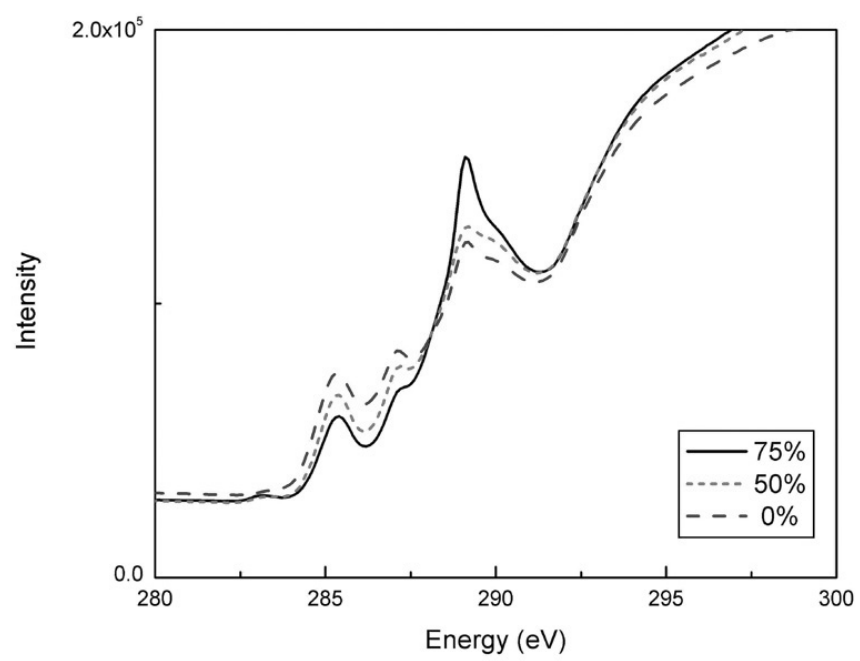


Figure 3

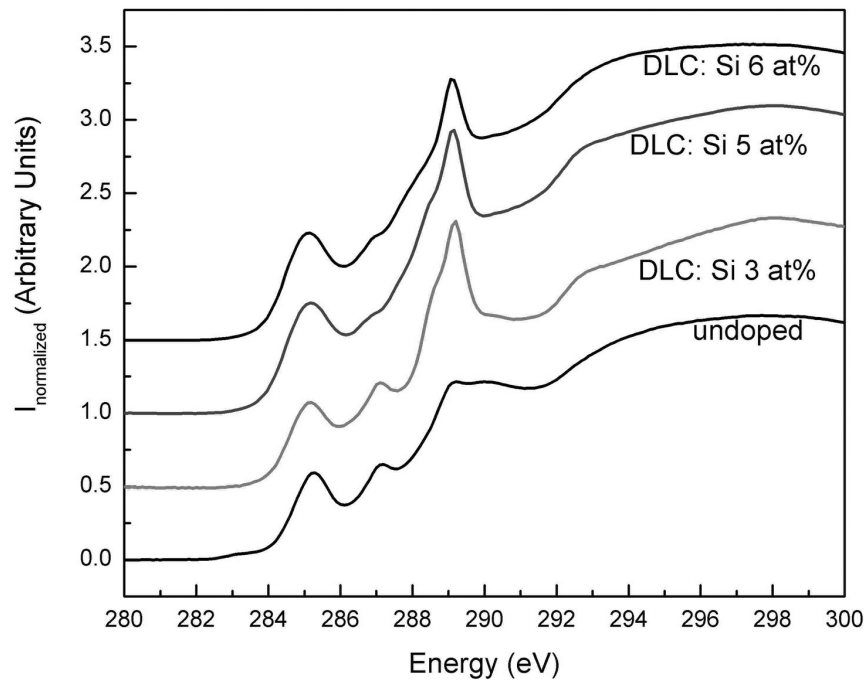


Figure 4:

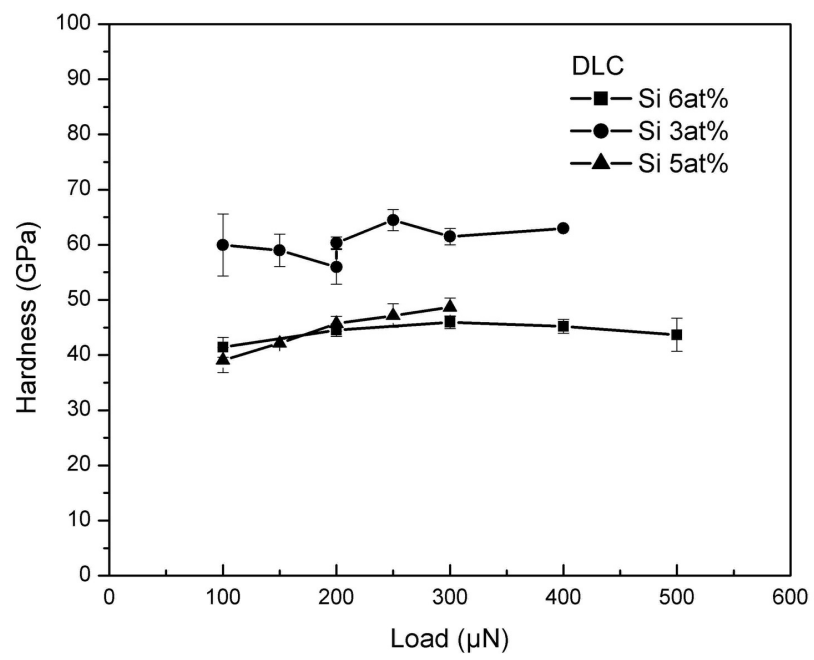


Figure 5

